Measurement and Modelling of Self-Heating in Piezoelectric Materials and Devices

Mark Stewart and Markys G. Cain

1 Introduction

There are many uses of piezoelectric ceramics where the desire for increased power output means increased drive levels, which subsequently can lead to thermal problems within the device. Applications such as:

- Ultrasonic Cleaning
- Ultrasonic Welding
- Sonar Transducers
- Diesel Injectors
- Ultrasonic Sewage Treatment

all use piezoelectric materials operated at high drive levels, where thermal loading on the device becomes an issue, and where potentially expensive cooling is needed to maintain device performance.

When piezoelectric materials are used as actuators they make use of the indirect piezoelectric effect, where the application of an electric field gives rise to an internal strain. In this solid-state energy transformation there will always be a balance between electrical energy input and work done by the device. The coupling coefficient, k, is used to describe this efficiency for an ideal case where there are no losses. Here, k is essentially the ratio of the open circuit compliance to the short circuit compliance. For most real piezoelectric materials this conversion process is also associated with losses—both mechanical and dielectric. These losses manifest themselves in the form of heat, causing a temperature rise in the device, which, depending on the thermal boundary conditions can be detrimental to device performance. This self-heating effect is most often encountered in resistive components and is termed "Joule

M. Stewart (✉) · M. G. Cain
National Physical Laboratory, Hampton Road, Teddington, Middlesex TW11 0LW, UK
e-mail: mark.stewart@npl.co.uk

M. G. Cain (ed.), *Characterisation of Ferroelectric Bulk Materials and Thin Films*,
Springer Series in Measurement Science and Technology 2,
DOI: 10.1007/978-1-4020-9311-1_7, © Queen's Printer and Controller of HMSO 2014

Heating". However, it is also seen in non-ideal dielectric materials where the dielectric loss gives rise to internal heat generation. To a first approximation, piezoelectric actuators can be thought of as a non-ideal or lossy dielectric but, because the material is moving, additional mechanical terms are needed to model this behaviour. If the energy loss to the surroundings is greater than the internal power generation, then the sample will eventually reach an equilibrium temperature. If the sample losses are greater than those to the environment, or if the losses increase with increasing temperature, then the sample will heat up until some catastrophic event is reached—such as the soldered connections failing, softening of adhesives, or depolarisation of the material.

There are several factors that limit the high power operation of piezoceramics in dynamic applications, such as sonar or ultrasonic welding transducers [1].

1. The dynamic mechanical strength of the ceramic
2. Reduction of the efficiency due to dielectric losses
3. Reduction in efficiency due to mechanical losses
4. Depolarisation of the ceramic due to the applied electric field
5. Depolarisation of the ceramic due to temperature rise.

The first can be largely overcome by correct prestressing or biasing of the ceramic, in order to limit large tensile stresses. The fourth factor, electric field, can be ignored for dynamic operations, since by the time this has occurred the field would be sufficient to cause failure by factors 2, 3 or 5. The most common causes are factors 2, 3 and 5, and the dominant factor depends on the type of operation.

1.1 Where Does Self Heating Occur?

In many cases this self heating does not present a significant problem, for instance in quartz crystals used for timing in electronics, the material's intrinsically low loss and the very low drive levels means that self heating does not adversely affect timing. However, in an ultrasonic humidifying unit, if the water reservoir is allowed to evaporate completely, they will fail due to overheating and for this reason they will usually have a cut out to prevent operation when the water runs out. Typically most self-heating related failures are in resonant continuous wave (CW) operation, since these are likely to be the most aggressive in terms of power input. However, even in non resonant operation, for instance in multilayer stacks where soft compositions are used, self heating can still be a significant problem.

1.2 How Does It Fail?

The self-heating can be benign, or it can manifest itself in several ways in the operation of a device. At one end of the scale, the changes in material and device parameters caused by the temperature rise will mean that a carefully designed resonant device will not resonate at the desired frequency. At the other end of the scale,

the temperature rise can be such that material itself fails through depoling, or through thermal stresses. Quite often, it is not necessarily the temperature rise in the ceramic that gives rise to failure, but the ancillary components that overheat and fail. For instance, solder may soften, insulation may breakdown, thermal expansion can lead to the release of prestress, and softening of adhesive leads to increased losses and failure. Tokin [2] state that "the main failures with multilayer piezoelectric actuators are deterioration of insulation resistance, short-circuit, and open-circuit". Although this need not be due to self-heating it can be a contributing factor.

1.3 Thermal Runaway

Much of the time, the phenomenon of self heating in piezoelectric materials is governed by linear processes and the temperature rise seen in a device reaches an equilibrium state, where the extraction of energy balances the internal energy generation through joule heating. It is possible, through positive feedback mechanisms, that the increase in temperature can lead to increased internal energy generation, leading to a rapid and uncontrolled temperature rise and subsequent failure. This phenomenon is also found in conventional capacitors [3] and is termed "thermal runaway", where the temperature dependence of properties can lead to positive feedback. Although thermal runaway is often associated with catastrophic failure, in Lead Zirconate Titanate (PZT) ceramic devices, failure is usually associated with the failure of ancillary components, such as soldered connections, adhesively bonded joints, etc rather than mechanical failure of the ceramic. If the temperature of the device approaches the Curie temperature, then the ceramic will become depoled, no longer piezoelectrically active, resulting in a failed transducer.

1.4 Examples

Figure 1 shows a typical failure in a high power ultrasonic transducer, which was probably caused by a failure in the insulating materials, as a result of the temperature rise, leading to dielectric breakdown and the catastrophic failure. The bunching of the wires together will exacerbate the overheating, due to decreased convection around the wires, and the pinning of the cables to the rear mass will also contribute to heating through mechanical strain.

Figure 2 shows a failure in a transducer from an ultrasonic cleaning bath. Evidence of thermal effects can be seen in the discolouration of the epoxy bonding the piezoelectric to the aluminium base plate. The cracking of the ceramic is very fragmented, indicating that the failure was not purely mechanical, but it is difficult to attribute the failure to purely a thermal cause without further investigations. The failure of high power devices involving epoxies is highlighted in 1–3 composites, where poor thermal transport away from the active ceramic causes temperature related failures in the epoxy resin [4].

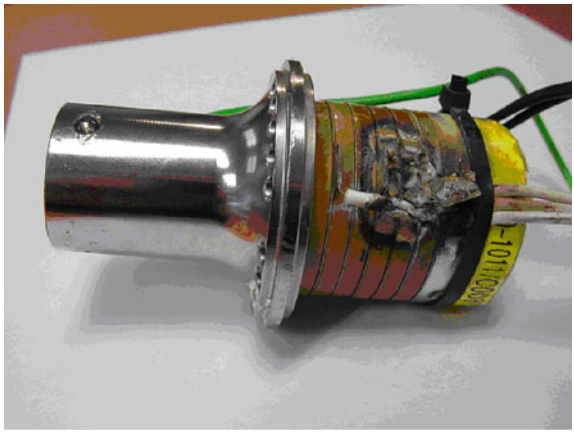

Fig. 1 Typical failure in a high power ultrasonic transducer

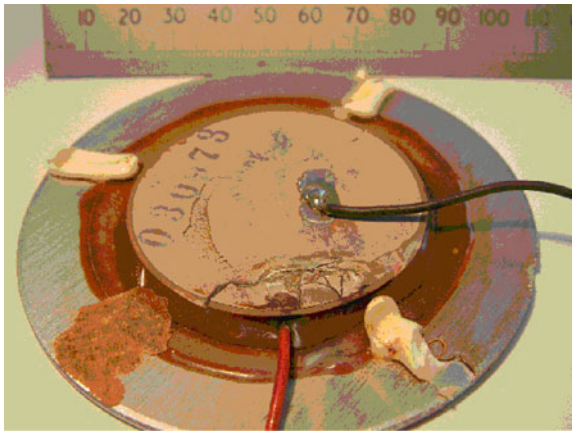

Fig. 2 Failure in a transducer from a laboratory ultrasonic cleaning bath

2 How to Minimise Self-Heating

This chapter is intended to help device designers to predict the effect of joule heating in their chosen device and its impact on device performance. If self-heating is a significant mechanism, then there are a number of ways that the problem can be lessened, most of which are common sense, although some may be less obvious.

Minimise Power input: The internal heat generation is dependent on the power input to the device and this can be limited by reducing the device operating conditions, such as driving frequency [5], field [6], or duty cycle. As many of the relevant material properties are non linear, a small decrease in power input may give a larger decrease in the heat dissipated in the device. Berlincourt [7] has suggested that for safe and efficient operation the dissipated power should be limited to less than 0.5 W/cm^3.

Maximise heat extraction: Obviously, the more energy that is removed through cooling processes, the less likely it is that self-heating will cause failure. This can

be achieved by adding heatsinks, forced air or liquid cooling. Conduction processes are usually most efficient at heat removal and increasing the gauge of the power leads will increase conduction and reduce resistive losses in the cable. Sometimes, the orientation of the device might help the convection process remove energy more efficiently. Hu et al. [8] found that by orienting a long vibrating plate vertically, rather than horizontally, the increase in convective heat removal, lead to almost a halving of the temperature rise.

Maximise device size: Many thermal problems within the microelectronics industry come from device miniaturisation, and if size restrictions can be relaxed, benefits in terms of thermal performance can be achieved. Since the temperature rise in a device can be controlled to some extent by the heat extraction, for a given power level a larger device will usually have larger, conduction, convection and radiation heat transfer paths. Uchino et al. [9] suggest for temperature rise suppression, a device with a larger surface area is to be preferred, for example a tube rather than a rod. Another approach might be to use a device designed for higher power levels, but drive it a smaller fraction of the maximum.

Include thermal safety cut outs: A thermal cutout is advisable, however it is not always feasible to measure the temperature of the ceramic itself if high voltages are involved or the device is resonant. In this case the temperature of a nearby component, or perhaps the air or coolant media can be measured, and a cutout based on this reading can be used. A less expensive option might be to prevent operation under certain conditions, for example without a coolant present, or when the device has been on for more than a certain length of time.

Reduce internal heat energy production by choice of material: As discussed in more detail later, the major contribution to the internal heating is dielectric losses in the material, so choice of materials with lower dielectric losses help to minimise internal heat generation. At a simple level this can be through selecting a hard, rather than soft PZT composition, since the hard materials have lower dielectric losses and can withstand higher operating temperatures because of their higher Curie temperatures. The selection is complicated by the fact that the dielectric loss is dependent on many factors such as driving field, compressive stresses and temperature. Berlincourt et al. [7] give several comparisons of efficiency depending on criteria such as, maximum internal loss limited to 0.5 $W/cm^3 \cdot kcps$, and a maximum tan delta of 0.04.

Reduce Mechanical Losses in the system: Although dielectric losses are usually the dominant source of heat generation, mechanical losses can also add to the overall heat generating processes. As we are considering an actuator, any motion in the device, apart from rigid body motions, has the potential to cause a stress and therefore a mechanical loss. It is often seen where the active material joins the passive components, and after all, this is how ultrasonic welding works. In 1–3 composite actuators, the active ceramic is in intimate contact with a passive epoxy, which often has a high mechanical damping coefficient, contributing to heat generation [10]. Where the electrical leads are soldered onto the active ceramic, stresses are introduced into the solder, which again will have a high damping coefficient. Hu et al. [8] have seen increased temperatures around solder joints on actuators, although they have attributed this to contact resistance, which can also contribute to heating.

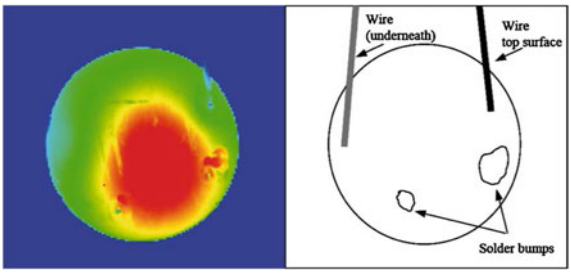

Fig. 3 Thermograph of self-heating in piezoceramic disc. Colour scale from *blue* (coolest) to *red* (hottest). Sample driven at thickness mode resonance of disc at 1.745 MHz. Coolest regions (*blue*) correspond to where power cables connect, and hottest points (*red*) to the two passive solder bumps

They suggest that making electrical contact at the nodal point, traditionally used to maintain a high Q in a device, may be counterproductive in terms of self heating, since this is where the strain transfer will be a maximum. Heating through mechanical losses can also be seen in the electrical contacts depending on how the wires are routed, often one end will be rigid and the other attached to the moving actuator.

Figure 3 shows the effects of solder connections on a disc resonating in the thickness mode at 1.745 MHz. The electrical power to the disc supplied via two soldered wires, one on the top surface, and one on the bottom. In addition to this, two extra dummy solder bumps that have been added to the top surface to examine the effect of these additions have on the temperature profile. The temperature of the device is non-uniform for several reasons. Although the sample is operating in thickness mode, non-uniform strains are still introduced through Poisson's ratio effects, which should lead to a temperature maximum at the centre of the disc. However because of the soldered connections, this maximum is offset towards the dummy solder bumps. The coolest parts of the device are where the power wires are connected; here the heat transfer through conduction in the wires leads to a smaller temperature rise. The two dummy solder bumps show increased temperature rise, probably because of the mechanical loss associated with the material. It is interesting to note that the solder joints associated with the power cables do not show the heating effect, since it is overshadowed by the increased thermal conduction in the cables.

In summary the contributions to the non-uniform self-heating in this device are in order:

1. Non-uniform strain in the soft piezoelectric material
2. Increased heat transfer through conduction in the power cables
3. Increased heat generation due to mechanical losses in the solder.

3 Measuring the Temperature of Piezoelectric Devices

When attempting to measure the temperature of piezoelectric materials used in actuators, there are several practical difficulties to be overcome. Firstly, the devices often have high voltages applied, which can have implications for safe and accurate

temperature measurement. Secondly, if the device is resonant, it may not be practical to attach contact temperature probes, since this will interfere with the resonant nature of the device. Thirdly, as discussed previously, when a moving actuator comes into contact with a passive (not moving) temperature probe, there is a potential for frictional heating, giving rise to erroneous readings. These three factors point towards using non-contact temperature measurement methods such as optical pyrometry, or even thermally sensitive paints. Thermally sensitive paints undergo a colour change, sometimes permanent, on reaching a certain temperature. The accuracy is limited, but they are cheap and essentially non-contact. If greater accuracy and range is needed and the temperature reading needs to be interfaced to data collection systems, then infrared (IR) temperature sensors are a reasonably economical solution. Errors can arise in these systems if the emissivity of the sample is low, or not precisely known, and the temperature measured by the radiation thermometer will not represent the true temperature of the sample. Also, if the sample is small, it might not be fully filling the field-of-view of the radiation thermometer, and the temperature measured will be an average of the sample and its surroundings. Occasionally the sample can act as a mirror and the sensor measures the radiation of an object from behind the sensor.

Another non-contact method of determining the temperature of a piezoceramic device is to use the temperature dependence of the material properties as a temperature indicator. The simplest property to use is the capacitance of the device. For instance a soft PZT-5H composition changes permittivity by 33 % over the temperature range 0–40 °C [1], and assuming this change is linear over the range, a change of 1 % in the capacitance represents roughly a degree centigrade. The measurement of capacitance could be realized using the device drive wiring and electronics, however it may be difficult to achieve the required accuracy, particularly when measuring hard materials, where the temperature dependence of capacitance is much less. Lente et al. [11] have shown a one to one correspondence between sample temperature and the polarisation during fatiguing of PZT discs. As the device fatigues, the change in polarisation causes a change in the current drawn by the device, leading to a change in temperature. Ronkanen et al. [12] have also identified the link between temperature and current drawn by the device, and suggest that this could be used a mechanism for compensation of output, as the change in temperature causes a change in piezoelectric properties such as d_{33}.

If contact methods are preferred, then there are several work-arounds that can be used to mitigate some of the problems discussed before. In order to mitigate the high-voltage danger, then the thermocouple can be placed on the ground side of the device, or a thin insulating varnish or cyanoacrylate can be used to attach the sensor. Of course, should the insulation or piezoceramic breakdown then there is a potential for damage to sensitive measuring electronics and also potential for hazardous voltages to come into contact with users. For this reason, it is advisable to have the temperature measurement electronics electrically isolated from the outside world. From the point of view of interfering with a resonant device and also in order to minimize ultrasonic heating effects, it is best to have very small temperature sensors that act as point sensors. In this respect, thermocouples are readily available

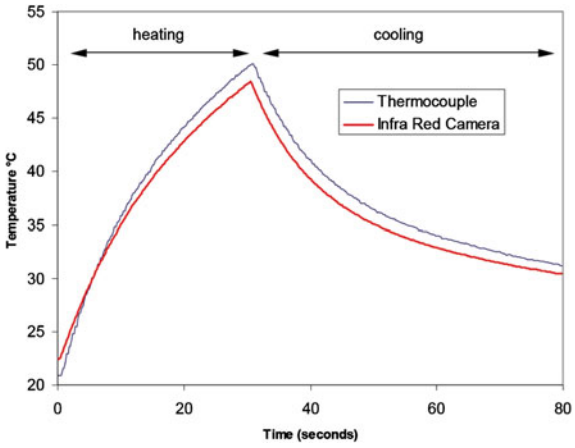

Fig. 4 Comparison of temperature measurements of a piezoceramic disc undergoing self-heating. Thermocouple is fixed to the disc with cyanoacrylate, IR measurements made with IR camera and temperature readings taken near thermocouple position

in thin wire gauges as small as 0.003″ (0.076 mm) diameter and smaller. Because of their low thermal mass, these small thermocouples are also advantageous in terms of their transient response and also their efficacy in measuring small samples reliably. Other contact mode sensors including Resistance Temperature Detectors (RTDs), thermistors and IC sensors, can all in principle be used, but the most commonly used sensors for these types of measurements are thermocouples and non-contact IR sensors. It should be pointed out that although no evidence of problems was seen in this work, there have been reports of thermocouples giving spurious readings in materials experiencing high power ultrasonic vibrations. Mignogna et al. [13] used copper constantan thermocouples bonded with epoxy to various resonant and non resonant bodies, and reported that the thermocouple would often record a temperature rise of as much as 100 °C, yet the sample was barely warm to the touch. Experiments to find the cause of these problems were inconclusive. However, they state "the results cast doubt on all previous measurements where thermocouples were used to measure heat generated during high-power ultrasonic insonation of metals". It should be stressed that the thermocouple measurements carried out in this work were used to record heating generated in the piezoceramic, and in general, temperature rise in the metallic parts was through heat conduction into the part, rather than internal heat generation in the metal.

Figure 4 shows a comparison of temperature measurements on a 30 mm diameter, 1 mm thick, disc of soft PZT, using a type K thermocouple and an infrared camera sensor. The thermocouple was attached near the centre of the disc using cyanoacrylate and the camera used gave a full field image of the device, but only results near the thermocouple position were used in the comparison. The IR system was corrected for emissivity of the target surface by placing the sample on a hot plate and comparing with the thermocouple readings. The calibration curve was highly non-linear, with a 4th order polynomial used to represent the readings, but this is probably a due to the camera sensitivity rather than the temperature dependence of the surface emissivity.

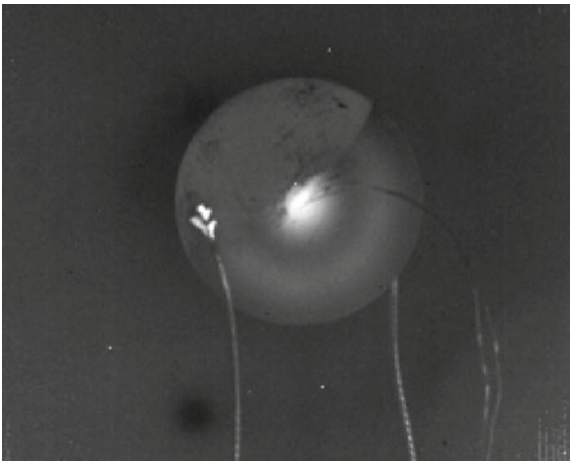

Fig. 5 Greyscale thermograph of PC 5H disc resonating in radial mode. Sample has been covered with graphite to give uniform emissivity, but then some of this coating has been removed to illustrate the effect of emissivity on the image. *Left hand* solder connection appears to be as hot as the *centre* of the disc. The *circular* pattern due to nodal strain heating effects is only visible on the graphite coated sector

The readings are a maximum of 2 °C apart and on average less than a degree apart, which is the order of the accuracy of the two systems. The differences could be because of the slightly different spatial positions of the sensors, (the disc was operating in a resonant mode so the temperature was spatially dependent), or because of the different time constants of the sensors. The fact that the two temperature traces cross on the heating cycle, but not on the cooling cycle could again be due to sensor time constants, or it could be due to electrical pickup. The only difficulty encountered in this work relating to thermocouple measurements came through electrical interference of a high power transducer running at around 1kW. In this case, when the power was applied readings shot to over 200 °C but instantaneously returned to ambient when the power was removed. The overall conclusion is, that thermocouple and IR sensors give identical results, except when substantial electrical interference is present, where these effects are easily identified.

The temperature sensors discussed so far have essentially been single point sensors. However, much information regarding the thermal performance of a piezoelectric device can be gained by using IR cameras. Calibration of these sensors is more difficult since the performance of each camera pixel could be different, however the information is usually used to detect differences point to point in an image and how this progresses in time. In this respect these types of images can often be misleading since the images will often contain areas with different emissivity that will be difficult to account for. Figure 5 shows a raw (uncorrected for emissivity) thermal image of a thin piezoelectric disc under resonant drive in the radial mode. To highlight the emissivity issue, one half of the discs top surface has a graphite coating, whilst this has been removed from the other half. The graphite gives an increased signal so it is possible to see the ring pattern produced by non-uniform self-heating, whilst this pattern is absent in the uncoated sector (uppermost). In the uncoated region the hottest part appears to be the soldered power connection, which is similar to the centre of the disc. In fact this is an artefact, the solder is acting as a mirror reflecting

some other part of the scene, giving a false impression of temperature. To overcome this the sample would normally be entirely coated with graphite.

4 Thermal Modelling

The aim of the modelling described here is to be able to predict the temperature rise in any piezoelectric device, given the sample type, applied voltage, frequency, and some environmental conditions.

4.1 Energy Balance

The temperature rise in a piezoelectric is a result of a change in its internal energy, and that internal energy can be found by an energy balance criteria, such that:

$$\text{Change in internal energy} = \text{energy generated in device} - \text{energy lost to surroundings}$$

Each of these energy transfer processes can be a function of many different processes:

$$\text{Energy generated in device} = f\ (\text{loss, frequency, capacitance, voltage})$$
$$\text{Energy lost to surroundings} = f\ (\text{conduction, convection, radiation}).$$

In order to model piezoelectric device behaviour as far as thermal conditions is concerned, there is a need to understand both the heat generation, and the heat transfer. The heat transferis a general problem that is covered by many textbooks and software solutions. There are many practical heat transfer problems that include internal energy generation, such as chemical reactions, nuclear radiation, resistive heating, where the solutions are common and the exact nature of energy generation process is not important. The mechanisms of heat generation in piezoelectrics, although similar to those in dielectric materials, are further complicated by the piezoelectric coupling. We will assume that the internal energy generation is the largest unknown in these problems and that the heat transfer constants are largely constant over the temperature range of interest for most cases.

4.2 Heat Transfer Processes

The three mechanisms of heat transfer; conduction, convection and radiation can be described by their individual rate law [14].

Conduction, the diffusion of energy by random molecular motion can be described by the rate equation, Fourier's Law.

$$q_x''(\mathrm{W/m^2}) = -\kappa \frac{dT}{dx} \tag{1}$$

where κ is the heat transfer coefficient for conduction, and has units of W/mK, T is temperature and q_x'' is the heat flux in the x direction.

Convection, which is a combination of conduction and energy transfer due to mass motion, advection, can be described by the following rate equation, sometimes known as Newton's law of cooling.

$$q_x(\mathrm{W/m^2}) = -h(T_s - T_\infty) \tag{2}$$

where h is the heat transfer coefficient for convection, and has units of $\mathrm{W/m^2K}$. Values for h can range from 2 for free convection in a gas, to 20 for forced convection, to many thousands for convection with a phase change.

Radiation, the transfer of energy by electromagnetic radiation, can be described by the following rate equation,

$$q_x(\mathrm{W/m^2}) = \varepsilon_m \sigma (T_s^4 - T_{sur}^4) \tag{3}$$

where ε_m is the emissivity, and σ is the Stefan-Boltzmann constant ($5.67 \times 10^{-8}\,\mathrm{W/m^2K^4}$).

In general the most important heat transfer processes for piezoelectric devices are conduction and convection. Since the devices are solid state the heat transfer within the device will be through conduction, and much of the energy transfer to the surrounding media will be through convection into air, water or other fluids.

4.3 Piezoelectric Device Operation

Piezoelectric devices are used in an ever-expanding range of applications that cover a wide range of operating regimes of frequency, power levels etc. However, as far as internal heat generation is concerned, there are three key types of driving conditions, resonant drive, non-resonant drive and non-CW drive.

Off Resonant Drive

In general, the temperature of the sample/ device is uniform throughout the sample. This is because strain throughout the sample is uniform, so each part of the sample volume is identical, apart from those that see a different heat transfer rate, such as sample surfaces or regions next to internal electrodes. It is usually accepted that under these conditions the dielectric losses contribute to self-heating. Several theoretical analyses have been developed to predict the temperature rise of devices under off resonant conditions. Most of these models assume that the thermal conductivity and

the heat generation mechanism are independent of temperature. Over the operating temperatures of most piezoelectric devices it is likely that the thermal conductivity is temperature independent, however the assumption that the internal heat generation is temperature independent may lead to underestimation of internal temperature profiles.

Resonant Drive

Here, standing waves are set up within the sample, which introduces a non-uniform strain and thus potentially non-uniform temperature. Non-uniform temperatures have been observed at nodal points in resonating devices [9, 15]. It is not clear if these non-uniform temperatures play a part in thermal runaway type behaviour. For example, a small part of the sample may become locally hotter and, through heat transfer, will heat up the rest of the sample. Here, the question arises: does failure come about from a small part reaching a critical temperature, or the whole sample reaching this temperature?

The critical factor under resonant drive conditions is that the mechanical loss is increased, and may contribute significantly to the internal heat generation, and also that this heat generation process is spatially dependent. Little work has been done on predicting temperature rise under resonant conditions, and the non-uniformity of temperature profiles.

Non CW Operation, Pulse Drive and Low Duty Cycle Operation

Non continuous wave (CW) drive waveforms of piezoceramics are often used, either because it is necessary for the particular operating pattern, or to overcome some of the overheating problems associated with CW operation. A diesel injector valve is an example of pulse drive, where the duty cycle is actually very small, but the operating cycle is very high power. In contrast, a high power ultrasonic cleaning bath may be a resonant device, but in order to restrain the temperature rise, the operation may be limited to duty cycles of 10 % or less.

For the ultrasonic bath example, the low duty cycle operation only slightly complicates the heat transfer problem, in that the heat generation is modulated in the time domain only. For the diesel injector example not only is the operation non continuous, the drive signal will likely be square wave, meaning that the internal heat generation will have many additional components in the frequency domain.

4.4 Modelling of Heat Generation

Dielectric Heating

In its simplest form a piezoelectric device can be thought of as a capacitive load, whose energy at any point can be modelled as the energy in a capacitor. If the capacitor

is not ideal then some of this energy will be lost, dependent on the dielectric loss tangent of the material. If we assume that all this lost energy is converted to heat in the capacitor through dielectric heating then the power dissipated can be given by Jordan and Quanies [16]

$$Power = 2\pi f C tan\delta V^2 \tag{4}$$

where f is the frequency, C the capacitance of the device, V the applied voltage and tan δ the dielectric loss. Dielectric heating is the mechanism for heating in a domestic microwave oven and the temperature rise of the food in an oven can be predicted similarly using (4), coupled with the density, specific heat capacity and the thermal boundary conditions.

Energy dissipation in piezoelectric materials is further complicated by the materials intrinsic non-linearity when driven under high field, such that the permittivity and dielectric loss become field dependent [17]. Coupled with this, the permittivity and dielectric loss will also be temperature dependent [18, 19].

The *dielectric heating model* has been used by many workers [20, 21] as a basis for heat generation in piezoelectrics driven at low frequency, under off resonance conditions. Uchino [9] used a modification to this model to predict temperature rise in multilayer piezoelectrics under off resonance drive. Uchino [9] expresses the rate of heat generation in the multilayer q as:

$$q = uf V_{eff} \tag{5}$$

where u is the loss of the sample per driving cycle per unit volume, f is the frequency, and V_{eff} is the effective volume of active ceramic material. The effective volume is dependent on the amount of active ceramic in a multilayer. The loss u is given by:

$$u = \pi \varepsilon^x \varepsilon_0 E_0^2 tan\delta_e \tag{6}$$

which is essentially a geometry independent version of the power loss in a capacitor seen previously [4].

Strain Heating

Under adiabatic conditions, a material undergoing a change in stress state can undergo a temperature rise in the same way that an ideal gas does. This temperature rise as a result of a volume change is termed the *thermoelastic effect* and can be described by the following equation:

$$\Delta T = \frac{\alpha_1}{\rho C_p} T(\sigma_1 + \sigma_2 + \sigma_3) \tag{7}$$

where α_i is the thermal expansion coefficient, and σ_i are the changes in the principal stresses. This temperature rise is fully reversible and results in cooling on expansion and heating on contraction. In practice these changes are of the order 0.1 K or less for fully elastic conditions in most metals. When the material is no longer perfectly elastic the material can undergo heating effects that are sometimes described as thermoplastic heating, and are attributed variously to grain boundary motion, dislocation movements, bond rotation in polymers and others. Here we will use the term, *strain heating* to describe the process of temperature rise due to mechanical motion in piezoelectric materials.

Under resonance drive conditions the dominant mechanism for heat generation is thought to be due to *strain heating*, rather than *dielectric heating*. This phenomenon is seen in many materials undergoing high power ultrasonic vibrations [13], and is mechanically analogous to dielectric heating. In dielectric heating there is a lag between the applied voltage and current, which corresponds to an energy loss, which is converted internally into heat. In strain heating there is a lag between stress and strain, and the corresponding energy loss is converted into heat. For dielectric heating the energy loss is proportional to the dielectric tan δ_e times the square of the field, whereas for strain heating, the energy loss is proportional to the mechanical loss, tan δ_m, times the square of the strain.

Ando [22] has used the following relationship to determine the mechanical loss for a given volume:

$$q_v = \frac{\alpha_v S^2}{2} \tag{8}$$

where α_v is the damping coefficient, and S the magnitude of the vibratory strain.

Other workers have used similar expressions using the applied stress, to describe the losses due to mechanical vibrations, [9, 23]. Uchino [9] determines the hysteresis loss in a full cycle using the following expression;

$$w_m = \pi s^E X_0^2 tan\delta_m \tag{9}$$

where s^E is the compliance and X_0 is the amplitude of the stress. Blotmann et al. [23] use a very similar expression, but divided by 2π, to define the mechanical dissipation, where the discrepancies with Uchino are due to imprecise definitions of the cycle. Lu and Hanagud [23], use irreversible thermodynamics to develop a model for self heating, but similarly show the strain heating is proportional to the square of the strain multiplied by various viscous damping coefficients.

The relationship between strain and heat generation implies that, under non-uniform strain conditions, for example at resonance or antiresonance, the heat generation will be spatially dependent. This is the key difference between strain heating and dielectric heating where, in the latter, the internal heat generation is assumed uniform throughout the volume.

Sherrit [24] has shown that for a plate sample of thickness, L and area A, with x=0 at the centre, the power distribution as a function of distance x is given by

$$P(x) = 2P_m \cos^2\left[\frac{\pi x}{L}\right] \tag{10}$$

where P_m is the mean power level. The cosine squared variation of temperature in a resonating piezoelectric device has been confirmed by Tashiro [15], although the form of the temperature variation at the fundamental resonance is not very different from a case with uniform heat generation. Several workers [25, 26] have modelled and measured temperature profiles of piezoelectric transformers driven at resonance, and shown that hot spots coincide with regions of high strain.

Dielectric or Strain Heating

In a capacitor the only internal heating mechanism is dielectric heating. However, for a piezoelectric material whenever an applied field leads to dielectric heating there will also be some associated strain heating. In general, most workers have assumed that under off resonance conditions dielectric heating is dominant, and ignored any strain heating contribution. Under non-resonant operation the induced strain will most probably be uniform throughout the sample, and because of this the errors associated with this will be equivalent to an error in the tan δ. Conversely, under resonant conditions the dominant mechanism is assumed to be mechanical heating, and dielectric heating is ignored [15, 24]. However, as before, where there is an applied voltage, there will be associated dielectric heating, but this will be spatially independent. Hu [25] has derived an expression for the internal loss per unit volume in a piezoelectric transformer as:

$$p(x) = A_0 \exp^{-\alpha x} \cos^2 kx + p_e \tag{11}$$

where the first term is the spatially dependent mechanical dissipation, and the second p_e is the dielectric heating contribution. As can be seen, neglecting this contribution will result in an offset in the temperature rise predicted, depending on the relative contribution of this second term. Determining the mechanical and dielectric loss for a given situation is difficult, and there are various approaches. Hu [25], uses the phase difference between the input voltage and current to determine the overall level of energy loss, and uses a value of 7:3 for the ratio of mechanical to dielectric loss, based on previous experimental evidence. Other workers [22, 23] use the low field values of mechanical and dielectric loss and Eqs. (6) and (9) to determine the individual contributions in FEA simulations.

4.5 Modelling of Heat Transfer

Steady State Heat Transfer

In the preceding discussion on heat generation, the power dissipatedwhen a certain sinusoidal field level is applied to a device can be determined. However, this is not a

means by itself to calculate the rise in temperature of a device. To achieve this, there must be some understanding of the material's thermal properties and the thermal boundary conditions of the device. At the simplest level we can imagine a volume of material that loses power P to ambient air, with a heat transfer coefficient h, (surface conductance into air), where the heat loss is essentially dependent on the surface area to volume ratio.

$$P = hT_m Area \tag{12}$$

Here P is the dissipated power and T_m is the temperature rise of the sample.

For a simple disc shaped device the surface temperature rise is given by [27]

$$T_m = \frac{P_v}{h}\left[\frac{2}{t} + \frac{4}{d}\right]^{-1} \tag{13}$$

where d and t are the diameter and thickness of the device, and P_v is the dissipated power per unit volume.

Equation (13) describes the surface temperature rise of a disc that has a uniform power generation P_v, and is losing energy to the surroundings via convection only. This assumes the temperature of the whole surface is the same, and the internal temperature is constant, i.e. the volume is small enough for internal heat conduction to be ignored.

The internal temperature, and it's spatial variation, of a plate, thickness L and area A, where the external temperatures are maintained at T_0, with a uniform internal power generation, P, is given by (Fig. 6).

$$T_x = \frac{P}{2kAL}\left[\frac{L^2}{4} - x^2\right] + T_0 \tag{14}$$

The external temperature T_0 can be determined by defining the control volume and the mechanisms of heat transfer in the media. However, to a first approximation T_0 is equal to the ambient temperature.

Equation (14) is valid for uniform power generation, and so would apply to off resonance drive, with dielectric heating. Sherritt et al. [24] have shown that if the power generation in the slab is not uniform, but proportional to the square of the strain, then the temperature distribution is given by:

$$T_x = \frac{PL}{2kA}\left[\frac{\cos^2(\pi x/L)}{\pi^2} - \frac{x^2}{L^2} + \frac{1}{4}\right] + T_0 \tag{15}$$

This distribution can be used to predict the temperature of a device driven at resonance, and so measurements of temperature distribution of resonating devices should be able to discriminate between dielectric heating and strain dependent heating. Figure 7 shows the predicted temperature distributions for uniform and strain squared heating, showing the different form of the behaviour. Unfortunately, if the

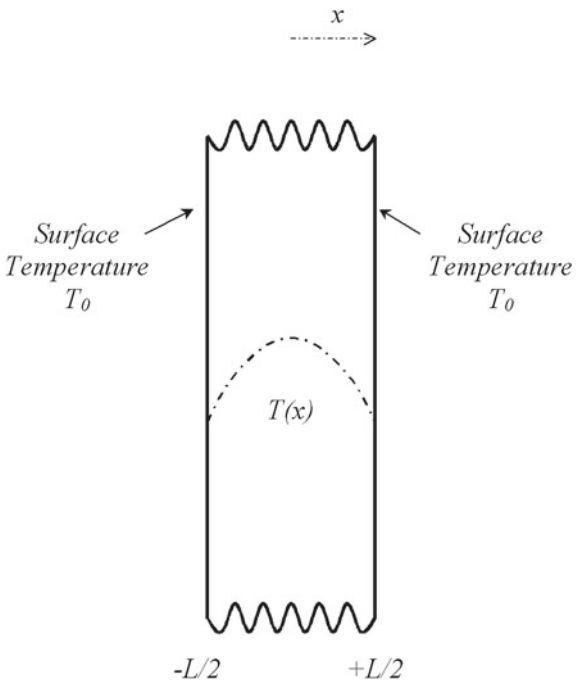

Fig. 6 Boundary conditions for analysis in Eqs. (13) and (14)

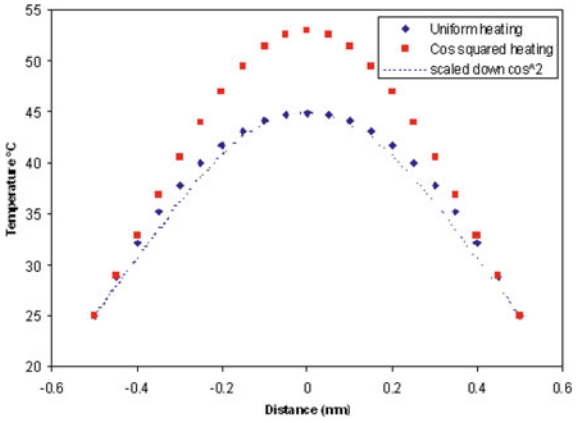

Fig. 7 Temperature profile of an infinite slab subject to internal heat generation. Comparing uniform heat generation with strain dependent heating

temperature scale of the cosine squared distribution is scaled down the behaviour is very similar to that in the uniform heating case, which means that very accurate experimental measurements are needed to definitively differentiate uniform and spatially dependent heating. As will be seen later the spatial dependent effects are more readily observed at the overtones than at the fundamental resonance of the device.

The preceding models only account for conduction in the sample. In order to account for convection at the surfaces the following model gives the temperature rise

at a distance x from an infinite slab of thickness L, with a thermal conductivity k, and heat transfer coefficient for convection, h:

$$T_x = \frac{P}{h}\left[\frac{L}{2} + \frac{h}{k}\left[\frac{L^2}{4} - x^2\right]\right] + T_0 \tag{16}$$

The maximum temperature is at the centre of the slab, x=0, and the minimum at the surface $x = L/2$.

Transient Heat Transfer

The models so far have covered steady state heat transfer, that is the predicted temperatures and temperature distributions are of a system in an equilibrium state, and it tells us nothing about the temperature change with time. In many applications, this equilibrium state is the most important, since this defines the steady state operating conditions. However, the knowledge of transient behaviour can be useful for low duty cycle behaviour, or for the prediction of thermal runaway.

The analytical solutions for transient heat transfer are much more involved than the steady state solution, and as a consequence the solutions are often numerical, based on finite differences or finite elements.

As an example the analytical solution for the temperature distribution in a semi-infinite solid, with initial temperature T_0, with heat produced at a constant rate P, per unit time per unit volume is given by Carslaw and Jaeger [28]:

$$T_{x,t} = \left[T_0 + \frac{\kappa t P}{k} + \frac{Px^2}{2k}\right] erf\left[\frac{x}{2\sqrt{\kappa t}}\right] + \frac{Px}{k}\left[\frac{\kappa t}{\pi}\right]^{1/2} \exp^{-x^2}/4\kappa t - \frac{Px^2}{2k} \tag{17}$$

where the surface is maintained at zero temperature, and κ is the thermal diffusivity.

Temperature Dependent Heat Generation

In all the previously described models the thermal material parameters and the heat generation processes have been considered temperature independent, with a consequence that all the solutions will be stable. From experimental results, it appears that the thermal diffusivity is relatively temperature independent and the thermal conductivity and specific heat capacity increase approximately 20 % over the common operating temperature regime. However the heat generation process is likely to be temperature dependent, as many of the dependent parameters such as dielectric constant and loss are also temperature dependent. Inclusion of temperature dependent heat generation can lead to unstable solutions, which is a possible mechanism for thermal runaway.

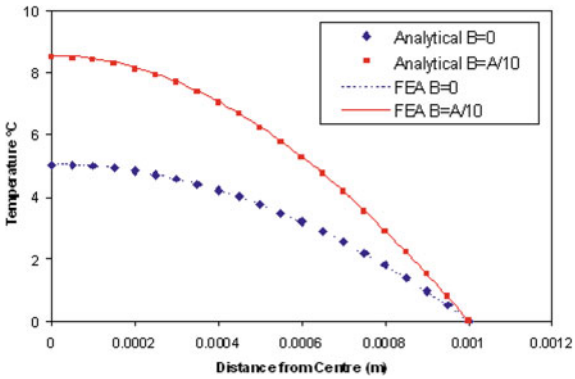

Fig. 8 Temperature dependent heat generation in an infinite slab, where B is the temperature dependent factor. Comparison of the analytical results (points) and a 1D finite element simulation (*lines*)

Adding temperature dependent heat generation to the models further complicates the solution and makes the analytical solutions even more complex. The following is the temperature profile of a slab length, l, with no flow of heat at $x=0$, and initial temperature of 0 K. The heat generation is defined by $k(A+B.T)$, where k is the thermal conductivity, $A$and B are constants where B is the temperature dependent part of the heat generation.

$$T(x,t) = \frac{A}{B}\left[\frac{\cos x B^{1/2}}{\cos l B^{1/2}} - 1\right] + \frac{16Al^2}{\pi}\sum_{n=0}^{\infty}\frac{(-1)^2 \exp\left[\left(-(2n+1)^2\pi^2 + 4B^2l^2\right)kt/3l^2\right]\cos(2n+1)\pi x/2l}{(4Bl^2 - (2n+1)^2\pi^2)(2n+1)} \tag{18}$$

In order for this solution to be stable, the temperature dependent part of the heat generation, B, must be such that the following inequality holds:

$$B < \frac{\pi^2}{4l^2} \tag{19}$$

If the equality holds then there is a steady state solution to the transient problem, given by:

$$T(x) = \frac{A}{B}\left[\frac{\cos x B^{1/2}}{\cos l B^{1/2}} - 1\right] \tag{20}$$

The temperature profile determined using Eq. (18) is illustrated in Fig. 8, calculated at long times, so it is equivalent to Eq. (20), and shows the effect of increasing the temperature dependent heat generation factor, B. Obviously the larger B becomes the higher the temperature at the centre will become, the outside temperature being held at zero in the model. To add other, more realistic, boundary conditions to the model,

the analytical solution increases in complexity, which is where FEA solutions come into their own. Also included on the figure are FEA solutions for the same problem, showing very similar results.

Finite Element Solutions

Finite element software such as ANSYS or PAFEC allows both transient and steady state solutions to heat transfer problems for a variety of boundary conditions, including internal power generation, temperature dependent thermal conductivity, and also some coupled field solutions, such as magneto thermal, i.e. the heat generated through joule heating in electromagnet coils. However, to model the self-heating problem observed in piezoelectrics using ANSYS, the temperature and piezomechanical solution would have to be solved sequentially. The thermal model would be treated as a system with internal power generation, and coupling between the piezomechanical and thermal solutions could be achieved through an iterative process.

Early work [29], using Finite Elements to model behaviour in an ultrasonic power transducer, used the dielectric heating model to determine the internal power generation, which was assumed uniform throughout the device. The dissipated power was determined by fitting results to experimental temperature profiles, rather than using the material dielectric loss and applied voltage to calculate the power.

Shankar and Hom [30], used dielectric heating alone to predict temperature related phenomena in an electrostrictive PMN sonar transducer. Contrary to PZT, dielectric loss in PMN decreases with increasing temperature [31], and so is not beset by the thermal failures seen in PZT. The internal power generation was calculated using the loss tangent and applied voltage, and this power distributed evenly through the device. In order to simulate pulse drive and reduced duty cycle, this power input was distributed temporally. For example, a 33 % duty cycle was simulated by full power on for 1 s, then off for 2 s.

Ando [22] carried out a comprehensive simulation of transient thermal behaviour in an ultrasonic transducer, using an iterative procedure as follows:

1. Determine the static stress and strain in the device
2. Calculate resonant frequency, stress, and strain etc using room temperature material parameters.
3. Determine the mechanical and dielectric heat dissipation.
4. Calculate heat diffusion and temperature distribution.
5. Calculate thermal stress, strain and thermal expansion.
6. Change material parameters due to new temperature distribution and repeat cycle.

This routine was continued until the required time was reached. He accurately predicted, not only the temperature rise of the device, but also its effect on the resonant frequency of the transducer.

Abboud et al. [32] have used the PZFlex finite element package to deal with heat generation in 1–3 piezocomposites. They point out that a coupled solution to the problem is difficult due to the different characteristic timescales of the different

processes; the piezoelectric vibration at 150 kHz, and the thermal conduction that occurs over the order of seconds. Their solution to this problem takes the following form:

1. Model the piezoelectric effect for one cycle and then calculate the power generation.
2. Solve for the transient thermal problem to determine the temperature distribution.
3. Apply any piezoelectric, mechanical, thermal property changes due to temperature rise/fall. Repeat steps 1–3.

The solution is reached at 2 when the temperature dependence of the material properties is negligible for the heating levels involved.

More recently Blottmann et al. [23], have performed a full 3D FEA simulation of model sonar transducers using ATILA. Mechanical and dielectric losses were included in the model, and although the mechanical loss was constant and the low field value, the dielectric loss was both field and temperature dependent. Again an iterative routine was used to modify material parameters dependent on the temperature rise from the internal losses.

Although fully coupled piezo-thermal solutions are not yet realised in FEA packages, another approach to the problem could be to use thermally dependent internal heat generation. In the ANSYS package, by using point elements, heat generation rates can be modelled using a polynomial of the form:

$$Q = A_1 + A_2 T + A_3 T^{A_4} + A_5 T^{A_6}$$

where the constants A_i can be input as "material parameters". Thus if it is possible to model the temperature dependence of the heat generation rate of the piezoelectric, this can be included in the thermal solution.

Example FEA Solution

As shown in Fig. 8, 1D FEA simulations agree well with analytical solutions but come into their own when the models become more complex.

Figure 9 shows a simple example of a 2D steady state FEA solution for a sample with uniform heat generation, and boundary conditions of 0° on the long sides, and held at 5° on the short sides. The temperature profile across the centre of the sample is similar to that in Fig. 8, however the core temperature is slightly higher because of the increased temperature of the short sides. This is relatively trivial example for FEA, however the 2D analytical solution would be much more complex.

5 Case Studies

In order to demonstrate some of the predictive modelling described in this document, a number of case studies will be discussed, where the models are compared to experimental measurements. Each case study is intended to highlight a different problem faced in modelling piezoelectric thermal behaviour.

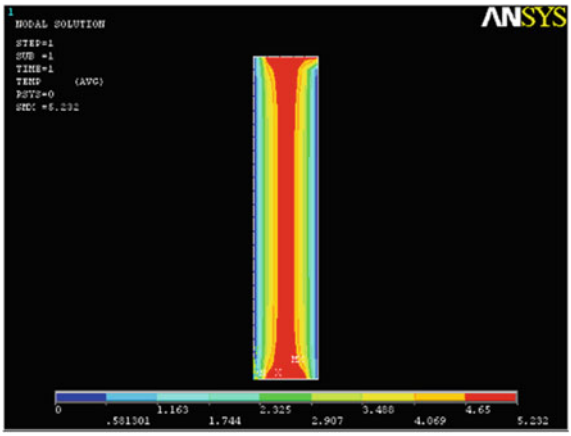

Fig. 9 2D steady state FEA solution for a sample with uniform heat generation. *Line* profiles are the same as Fig. 8, but the end effects are observed because the slab is not infinite

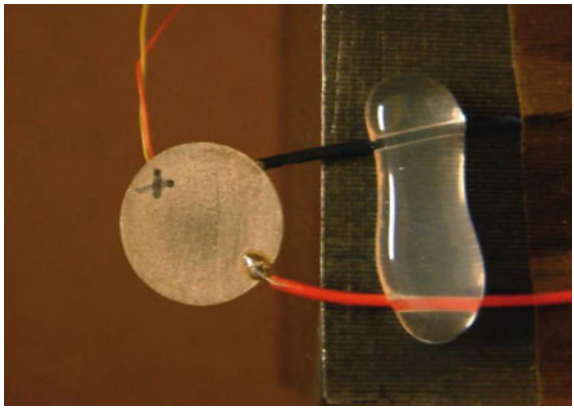

Fig. 10 PZT disc sample, suspended in air, showing power cables (*thick*) wires and thermocouple (*thin wire*)

5.1 Case 1: Off Resonant Drive of a Simple Monolithic Ceramic Disc Suspended in Air

Rationale: This is almost the simplest case encountered; the sample is thin, so there is no significant temperature profile through the sample. A balance between internal heat generation, and heat removal via convection from the surface, governs the sample surface temperature and there is no thermal conduction. The sample is operating off resonance, so the internal heat generation is assumed uniform throughout the sample.

The sample is a 0.2 mm thick, 10 mm diameter disc of soft PC 5H composition, mounted as shown in Fig. 10. The sample was placed in a large enclosure, approximately $0.03\,m^3$ (1 cubic foot), to control the air movement around the sample. The temperature of the sample was measured with a thermocouple, and comparisons were made using an IR sensor, but little difference was seen. The sample was driven bipolar at frequencies of 100 Hz–5kHz and the current and voltage measured during

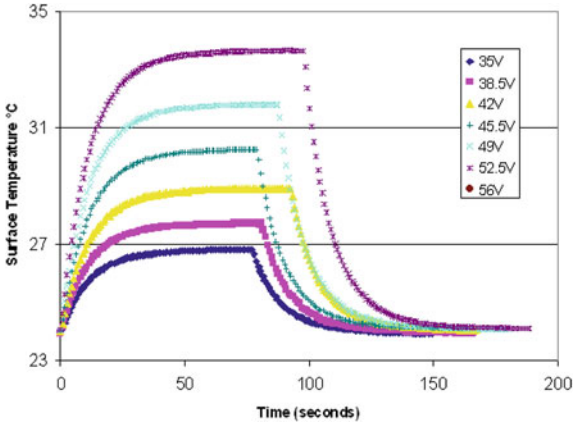

Fig. 11 Example heating/cooling curves for a thin piezoelectric disc driven at 5 kHz. Power is automatically cut off when sample temperature stabilises, resulting in cooling curves

each run. The data collection routine had a thermal cut-off point, should the sample surface temperature reach 100 °C, in order to prevent irreversible changes in the material. Otherwise the applied power would be automatically removed once a stable temperature was reached.

Figure 11 shows an example of heating/cooling curves for these experiments, for applied voltages at 5 kHz, where generally the self-heating leads to an equilibrium temperature. The equilibrium temperature depends on a number of variables including the geometry, convection coefficient as well as voltage and frequency, but as stated previously is essentially a balance of the input energy against the energy removal processes. This balance can be described by the following equation:

$$E_{st} = E_g - E_{out} \tag{21}$$

where;
E_{st}= Energy Stored in Sample with temperature rise via Cp (equation (A1))
E_g= Internal Energy Generation via dielectric Heating (Eq. 4)
E_{out}= Energy Removal via convection (Eq. 2) or radiation (Eq. 3).
As the sample is operating off resonance, the internal energy generation can be calculated using the dielectric heating model, Eq. (4). The thermal energy stored in any arbitrary block of material can be determined from Eq. (28), and assuming there is no thermal conduction, the energy removal can be determined from Eqs. (2) and (3).

Assuming that there are negligible heat losses from the edge of the disc, the instantaneous temperature rise is given by

$$\Delta T = \frac{2\pi f \varepsilon \varepsilon_0 V^2 \tan\delta / t - 2h(T - T_{amb}) - 2\varepsilon_m \sigma (T^4 - T_{sur}^4)}{\rho t C_p} \tag{22}$$

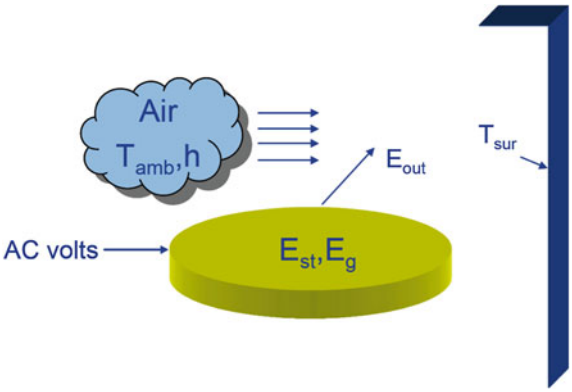

Fig. 12 Schematic of energy balance in self heating of piezoelectric disc

where t is the disc thickness. The terms in Eq. (22) are a mixture of material parameters, fundamental constants and experimental conditions, where the least accessible value is the convection coefficient, h. The convection coefficient is very dependent on experimental conditions and although it can be estimated it can also easily be determined experimentally from the cooling curves.

Newton's Law of Cooling

Newton's law of cooling simply states that the rate of change of the temperature is proportional to the difference between its own temperature and ambient, where the proportionality constant is the heat transfer coefficient, h.

$$\frac{dT}{dt} = -h(T - T_0) \tag{23}$$

Solutions to this equation take the form:

$$T(t) = T_{amb} + (T_0 - T_{amb}) \exp^{-ht} \tag{24}$$

This simple equation can be used to model many thermal problems, such as cooling cups of coffee, time of death calculations, and also thermal behaviour of piezoelectric devices. Several workers [33–35] have used this model to fit to experimental data of surface temperature changes of self-heated piezoelectric devices, and although the heat transfer coefficients obtained are dependent on specific device geometry and boundary conditions, it does permit limited predictive capabilities.

A value of 33 W/m^2K for the heat transfer coefficient gives a good fit to the experimental cooling curve, Fig. 13. Strictly speaking, this constant applies for the cooling curve, and it is possible that it may not necessarily be equivalent to the heating process. Zheng et al. [33] has attributed variations in heat transfer coefficients in active piezoelectric devices, to the increased convection due to the vibrating surface.

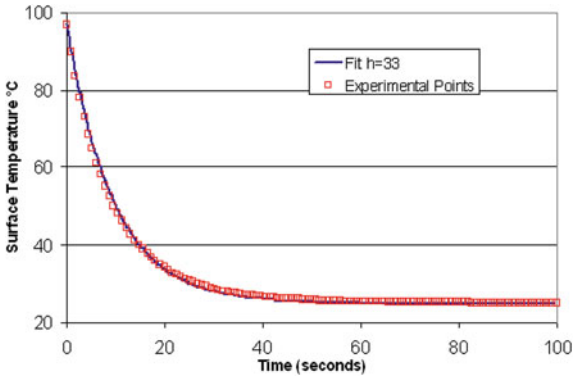

Fig. 13 Cooling curve of thin piezoelectric disc with experimental fit based on Newton's law of cooling

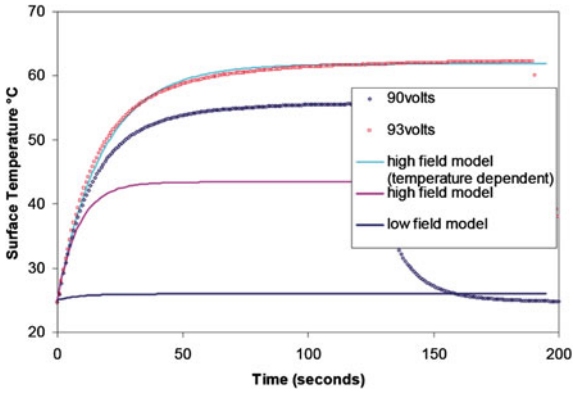

Fig. 14 Experimental results of self heating of thin piezoelectric disc driven at 500 Hz, compared with "low field" and "high field" models based on Eq. (22)

Model Assumptions

The model described by Eq. (22) has a number of assumptions including; negligible heat losses from the disc edge, uniform temperature throughout disc, radiation occurs between a small sample and large enclosure, and most importantly constant material properties, i.e. temperature invariant.

As an example the model is tested on heating curves when the sample is driven at 5 kHz, with an applied voltage of 93 V. If the model is used with the typical material constants, in particular the "small signal" or "low field" permittivity and loss values, this gives us a very poor fit to the experimental results. In the "low field" model the values used for permittivity and loss are 2600 and 0.02 respectively, leading to an overall temperature rise of 1 °C, Fig. 14. It is perhaps unrealistic to use the "small signal" dielectric constant values, since small signal is generally measured at fields of around 1 V/mm. If the dielectric constants measured at a "high field" of 94 V are used, permittivity = 3300 and loss = 0.3, then a stable temperature rise of 18.5 °C is predicted. The "high field" model is improved compared with the "low field" prediction, however the temperature rise is roughly half that measured.

The assumption in the model so far has been that all the material constants are temperature independent, however this may not be a valid assumption. The dielectric properties, particularly for soft materials are known to be temperature dependent, and measurements of the voltage and current during the experiment have shown this to be the case. The temperature dependence can be included in the model by assuming a linear variation with temperature for the permittivity and loss such that;

$$\varepsilon = 3300 + 70 * (T - T_{amb}) \tag{25}$$

$$\tan \delta = 0.3 + 0.001 * (T - T_{amb}) \tag{26}$$

A much improved fit is obtained when the temperature dependence of the dielectric properties is included in the model, Fig. 14.

Thermal Runaway

As discussed previously, thermal runaway occurs in systems when the internal energy generation is greater than the energy removal rate and the system becomes unstable, usually ending in system failure. It is common in chemical processes, charging of batteries and capacitors [3], many semiconductor devices, as well as piezoelectric devices. The key feature of this phenomenon is some kind of positive feedback between the internal energy generation and the increasing temperature.

Initial internal heat generation rate
⇓
Increases temperature
⇓
Increases heat generation rate
⇑

From the modelling of the thin disc it is clear that the temperature dependence of the dielectric properties plays a key part in temperature rise and is a possible mechanism for this positive feedback.

When the disc is driven with high fields at a higher frequency of 5 kHz, the sample starts to exhibit thermal runaway, Fig. 15a. This can be seen more clearly as a change in the temporal temperature gradient from negative to positive, Fig. 15b. In this case at a voltage of approximately 84 V the behaviour changes from stable equilibrium temperature to thermal runaway. This behaviour is chaotic and the exact voltage that this change occurs is highly dependent on slight changes in the experimental conditions such as the heat removal rate. Figure 15a also shows the modelled temperature rise (solid lines), based on the temperature dependent high field model. The fit for the higher voltages, cf. 91 V, is not as good as at 77 V and reflects the chaotic nature of the behaviour near the runaway point. In order to get a better fit at 91 V it is necessary to raise the modelled voltage to 100 V.

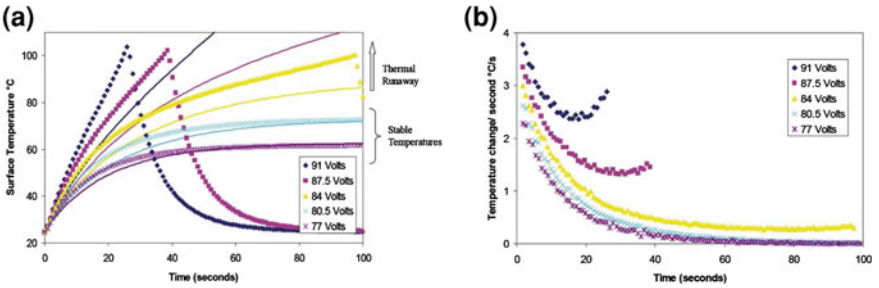

Fig. 15 Self heating in a thin PZT disc driven at 5 kHz exhibiting thermal runaway. **a** Experimental temperature rise (points) and modelled temperature rise (*solid lines*) based on a temperature dependent high field model. **b** Rate of temperature change of disc showing clearly the onset of thermal runaway. Power is automatically cut off when sample temperature stabilises, or temperature reaches 100 °C, resulting in cooling curves

Conclusion

A simple model based on the energy balance in a volume, where only energy generation, convection and radiation are considered has been developed that can accurately predict the temperature rise in thin piezoelectric discs. It has been shown that this model is vital if the internal heat generation mechanism is temperature dependent, and it can even extend into prediction of thermal runaway, although here the chaotic behaviour make accurate predictions difficult. The model is solved iteratively, and in principle this method can be incorporated into FEA solutions where complex geometries and thermal conduction can be included.

5.2 Case 2: Resonant Drive of Simple Monolithic Ceramic Suspended in Air

Rationale: This device was chosen to illustrate the effects of the spatially dependent heating of a piezoelectric, depending on the strain profile at resonance. The device has a large surface area to fill the field of view of the thermal camera, and is driven in the d_{31} mode, so the direction of electric field is perpendicular to the expected spatial thermal anomalies.

Experimental

A bar of hard PZT 4D material, 70 mm long, 10 mm wide and 2 mm thick is driven at longitudinal resonance and its overtones. The bar is poled across the width and the field is also applied in this direction, resulting in expansion along the length. The sample is driven at the resonance frequency, 24 kHz and the first and second

overtones, 71.2 and 111.1 kHz. The sample is suspended in air on two wooden cocktail sticks, and thermal images recorded using an infrared camera. The temperature readings from the camera were corrected for emissivity by placing the sample on a hot plate and comparing the camera results with those from a type K thermocouple.

The thermal images, Fig. 16, clearly show different behaviour dependent on the resonant mode. At 71.2 kHz the first overtone of the length resonance, there are clearly three hot spots along the length, roughly coincident with the nodes where the strain is at a maximum. Similarly at the second overtone, 111.1 kHz, there are five hot spots and seven cool areas. The power cables also appear to heat up, being hotter where the wire makes contact with the bar. Some of this could be due to contact resistance as the silver electrode did not make good mechanical contact and was sometimes pulled off with the wire. Ideally the centre line scans should be perfectly symmetrical, however there is some evidence that the right hand side of all the images are nominally hotter. There are several possible reasons for this, including misalignment of the sample, uneven illumination of the sample and non-uniform pixel array sensitivity.

Modelling

The modelling of the resonator was performed using a 3D thermal FEA model, consisting of brick elements with eight nodes, with a single degree of freedom, temperature, at each node. This element was used for both, steady-state and transient 3-D thermal analysis. The heat loss from the resonator was through a uniform convection coefficient on all the surfaces, conduction through the wires and supports and radiation loss was ignored. The convection coefficient was determined by matching the predicted cooling curves to the measured temperature and a value of 10 W/m^2K was used.

The heat generation was modelled by distributing the dissipated power according to the square of the strain, since both tensile and compressive strains lead to a temperature rise. In the d_{31} mode the largest strains occur along the length, x direction, and the strain in the other directions was assumed to be uniform. Therefore the dissipated power was distributed according to the following equation:

$$P(x) = P \sin^2 \left[\frac{n\pi x}{L} \right] \tag{27}$$

where P is the power per unit volume, L is the sample length, and n depends on the resonant mode, odd for resonance and even for antiresonant modes.

Figure 17 shows the measured centreline temperature profile after 50 and 100 s and the transient modelled profiles using n=3 and a power level of 0.2 W/cm^3. The model shows the same peaks and troughs as the real behaviour, and this holds for different times, however the match is not perfect. The fact that the measured profiles are hotter towards the right hand side has already been discussed, however the central point is consistently the hottest part on the measured device, a feature that is not mirrored in the model behaviour. It is possible that the electrical contacts, which

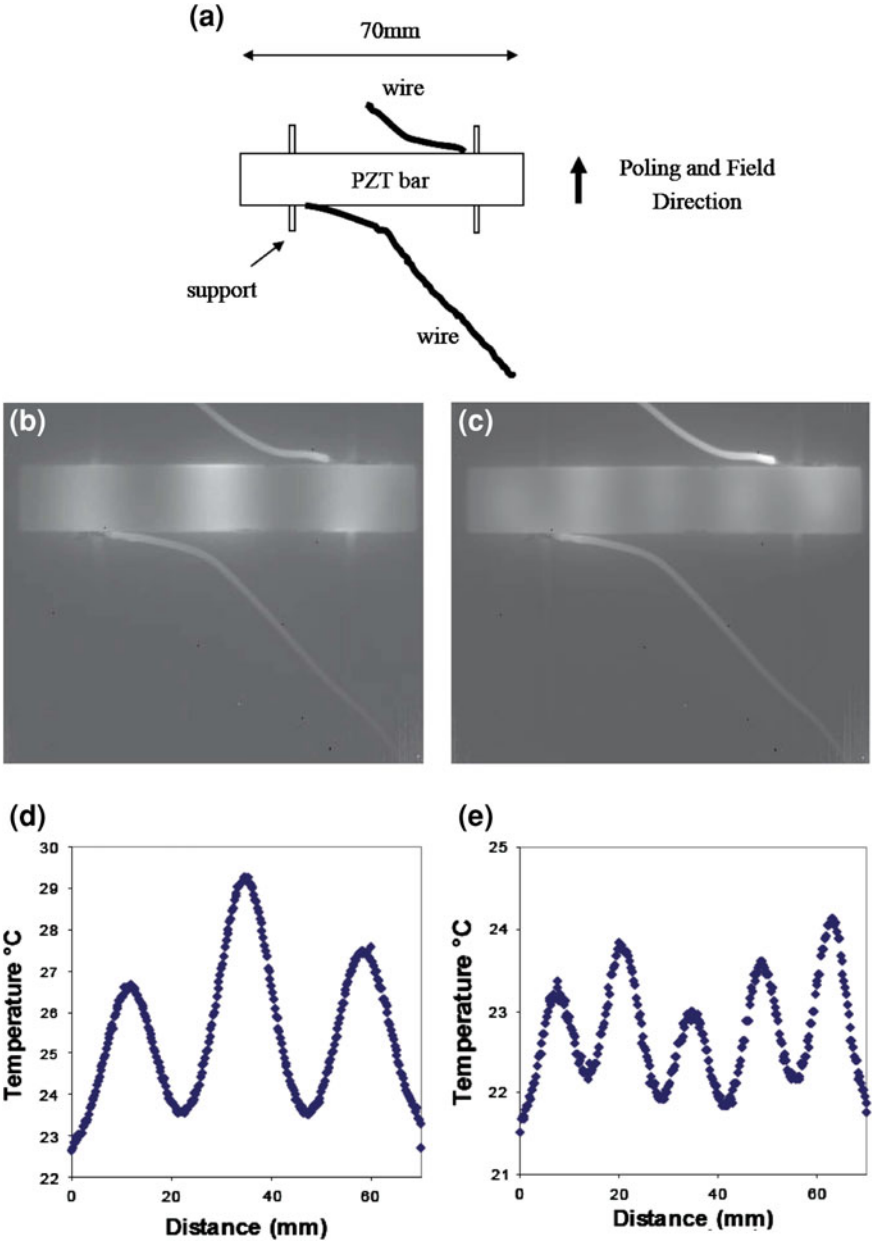

Fig. 16 **a** sample setup, **b**, **c** Thermal images of piezoelectric bar driven at resonance. **d** Thermal image and centreline temperature profile of first overtone, 71.2 kHz. **e** Thermal image and centreline temperature profile of second overtone, 111.1 kHz

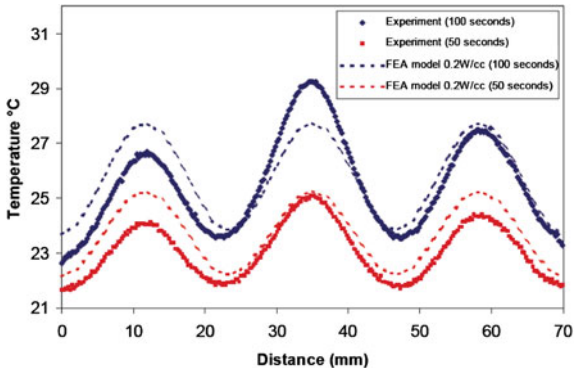

Fig. 17 Experimental and modelled temperature profiles for a bar driven at the first overtone 70.2 kHz

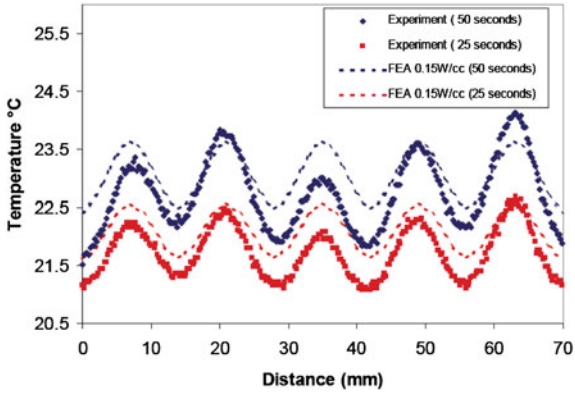

Fig. 18 Experimental and modelled temperature profiles for a bar driven at the second overtone 111.1 kHz

are coincidentally near the side lobes are the cause of increased heat loss through conduction.

The modelled and measured temperatures for the second overtone, $n = 5$, are shown in Fig. 18. As can be seen, the temperature difference is smaller for this mode, because the strain variations are closer together. The model still gives a reasonable representation of real behaviour, but now because of the small temperature rise, the errors in the measurements are more apparent.

So far, the results of the model have shown the temperature profile of the centreline of the top surface only. The FEA model is 3D, so it predicts the temperature of the entire sample, and the surface temperature is shown in Fig. 19. From this it can be seen that the predicted temperature is not uniform along the width direction and the contours around the hot spots are convex, whereas around the cool areas they are concave. This is due to the thermal edge effects where more heat is lost near the edges because the material in this region is close to two surfaces. In fact, the experimental behaviour shows the opposite, with the hot spots being concave, and the cool areas convex. In the model we have assumed that the spatial dependent effects are entirely in the x, length direction and uniform along the width, y direction. In fact, because

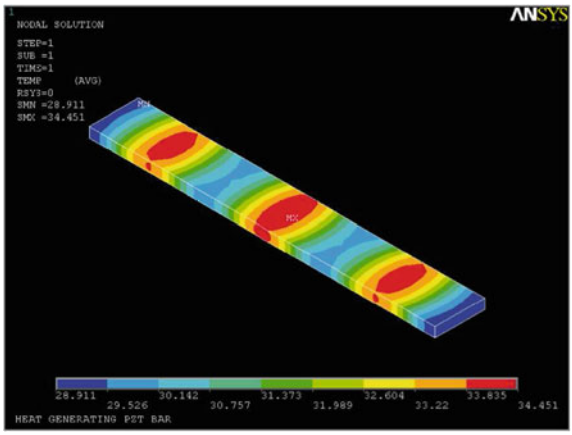

Fig. 19 Full 3D FEA simulation of temperature map of bar where n=3, first overtone

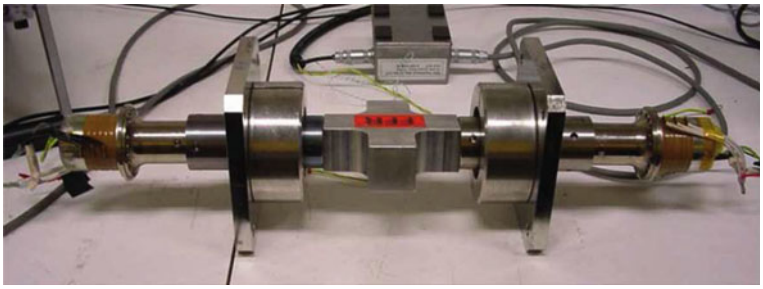

Fig. 20 Photo of the back to back high power transducer system

of mechanical edge effects, the strain levels near the edge decrease, which would amplify the thermal edge effects, thus increasing the curve of the contours rather than reversing them. Although the predicted contours take the wrong form, in practice the errors in actual temperature levels are less than 0.5 °C.

Conclusion

The case study clearly illustrates the spatial dependence of heat generation in a piezoelectric device driven at resonance. This behaviour can be modelled by assuming a sine-squared distribution of the power dissipation rather than a uniform one. The effects here are dramatic because the resonator is mechanically and thermally well insulated. In many practical situations the resonator will be attached to another medium and heat transfer through conduction will override the spatial dependent effects seen in this case.

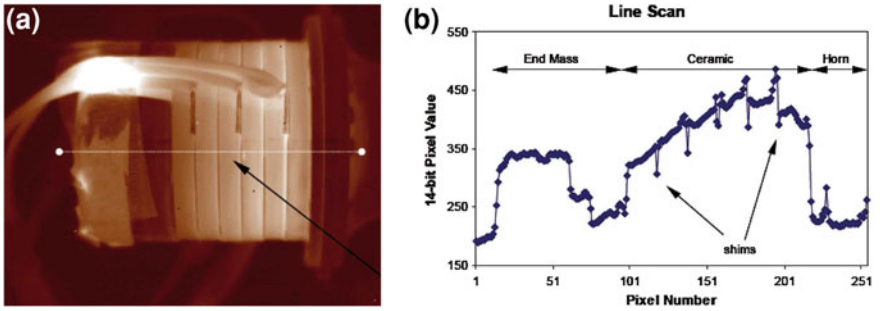

Fig. 21 Thermal image of high power transducer driven at an input power of 400 W for 400 s, with associated line scan pixel values

5.3 Case 3: Resonant Drive of a Clamped Ceramic (Bolted Langevin Transducer)

Rationale: This is an example of an industrial high power transducer and includes all the problems associated with non-ideal cases. The device geometry is more complicated, there are many different materials present, and the drive electronics are proprietary. Because of these complexities, it is no longer viable to solve this using analytical solutions and finite element methods must be used.

Experiment

The transducer is a commercial high power device, and in order to drive the system safely at high powers it is necessary to extract power from the system. This is achieved by mounting two transducers back to back in the form of a 1:1 piezotransformer, where the output is terminated into a resistive load consisting of several halogen lights. Figure 20 shows the system, which is held horizontally at the nodal points by two large steel plates. The transducers have a resonant frequency of 20 kHz, and the active piezoelectric consists of 6 rings of PZT, 5 mm thick and 50 mm OD, stacked sequentially but wired electrically in parallel. The ceramic is prestressed by a stainless steel back mass using a high tensile steel bolt which is attached to the aluminium front horn. The ceramics have silver electrodes, but in order to make a mechanically robust electrical contact to these a thin metal shim is placed between each PZT disc. These shims have a small tab to enable the electrical contact to be made.

The temperature of the transducer was measured with an Indigo Merlin InSb mid range infrared camera with a 320 by 256 pixel array. Figure 21 shows a greyscale thermal image of the device after being driven for 400 s at an input power of 400 W. The image shows hot spots associated with the three power cables, and also close to the metal shims. The hot spot where the cables are bunched together is real, i.e. this is the hottest part of the cables, but not necessarily the hottest area in the image.

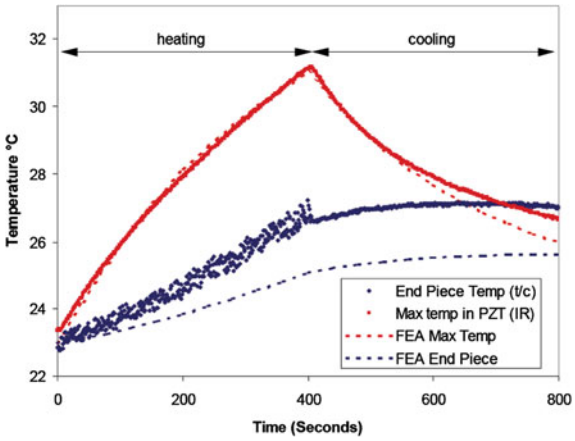

Fig. 22 Measured temperatures during application of 400 W electrical power for 400 s. *Red*, maximum temperature measured using IR camera, *blue* temperature measured using thermocouple attached to back mass of transducer. *Dashed lines* show FEA predictions based on 5 W power dissipated

The hot spot close to the left hand side of each shim is an artefact, where a small raised portion of the shim is reflecting radiation from some other part of the scene. This illustrates the necessity for emissivity correction. The camera gives a 14-bit number associated with each pixel, and this must be corrected for the emissivity of the object in order to convert this number to a temperature. The emissivity correction was carried out for the PZT only, by heating a similar piece of PZT on a hotplate, attaching a thermocouple to the surface and comparing the results. Because of the high voltages present it was not possible to attach a thermocouple to the active part of the transducer, but a thermocouple was attached to the steel back mass, roughly half way along the length. For ease of data capture only a line scan was captured every 200 ms, and the data for the line is also shown in Fig. 21. In order to get an idea of the transient behaviour, the maximum temperature in the ceramic and the temperature from the thermocouple are plotted in Fig. 22. A power of 400 W was applied for 400 s and then turned off, whilst still measuring the temperature. The thermocouple shows the effects of electrical pickup whilst the power is applied, but this noise is still only around 0.5 °C. It is interesting to note that temperature of the end mass still continues to rise after the power has been removed before eventually cooling down.

FEA Modelling

The modelling of the transducer was carried out by simplifying the device to an axisymmetric system, consisting of three thermal elements, the steel back mass, aluminium horn, and the active ceramic ring. The values used for the thermal properties for the elements are listed in Table 1. The heat loss from the device was assumed to be through convection only, since at these temperatures energy dissipation through radiation is small. All the external surfaces were subject to a uniform heat transfer coefficient, with the air temperature maintained at ambient. The value of this coeffi-

Table 1 Thermal properties used for FEA model of transducer

	Density (kg/m^3)	Thermal conductivity (W/m K)	Specific heat capacity (J/kg K)
Steel	7,800	75	640
PZT	7,500	1.2	320
Aluminium	2,700	200	900

cient was estimated by matching the predicted cooling curves to the measured and a value of 3 W/m^{2}K was used. The convective heat transfer coefficient is probably the biggest source of error in the analysis, since it is unlikely to be completely uniform due to the complex geometry of the system. However even with this assumption the model shows all the features found experimentally.

If we assume that the internal heat generation can be modelled by the power dissipated through dielectric loss then for an applied voltage of 1000 V and using a relative permittivity of 1300 for the material, this leads to a power of around 10.9 W for a tan delta of 0.2. If this power is uniformly distributed over the volume, then this leads to a power/unit volume of around 220, 200 W/m^3, or 0.22 W/cm^3, which is within the safe rule of thumb value of 0.5 W/cm^3 given by Berlincourt [7]. Figure 23 shows the predicted temperature rise of the model after 400 s at a power level of 10 W, where the maximum temperature is at the centre of the PZT. The model matches the transient behaviour reasonably well for different power levels, Fig. 24. Halving the power input in the model to 5 W agrees well with the experimental measurements. The model also predicts the temperature rise in the rest of the transducer, but the matching between the measurements taken by the thermocouple on the back mass and the modelled behaviour is not as good, Fig. 22. The form of the predicted behaviour is very similar, it predicts the slight temperature increase after the power is cut, but the measured temperature rise is roughly 2 °C greater than predicted. This is probably because the thermocouple was attached to the transducer using kapton tape, which had the effect of insulating the thermocouple from the surrounding air.

In order not to overheat the transducers the maximum operating time was limited to 800 s, however the thermal model predicts that steady state will be reached in around 12 h, where the maximum temperature for the 5 W dissipated power would be 100 °C and for 10 W, 180 °C.

The transducer is a resonant device; therefore it is perhaps unreasonable to assume that the internal heat generation is uniform throughout the device. At the fundamental resonance the strain in the transducer is distributed such that there is maximum strain in the ceramic directly next to the titanium horn, and it decreases sinusoidally to zero at the end of the device. If is assumed that the power distribution of 10.9 W is distributed according to the square of this strain, rather than a uniform distribution, then this should lead to a more accurate prediction of the temperature. The predicted temperature for uniform and strain heating are shown in Fig. 25 along with the measured temperature in the ceramic. As can be seen the strain dependent temperature profile is shifted slightly towards the point of maximum strain, but in fact there is very

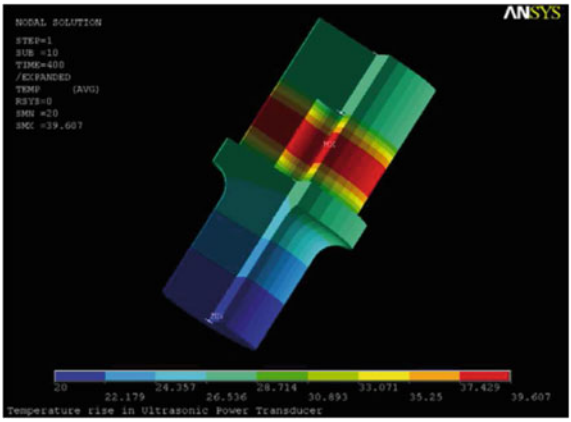

Fig. 23 Thermal FEA model of high power transducer

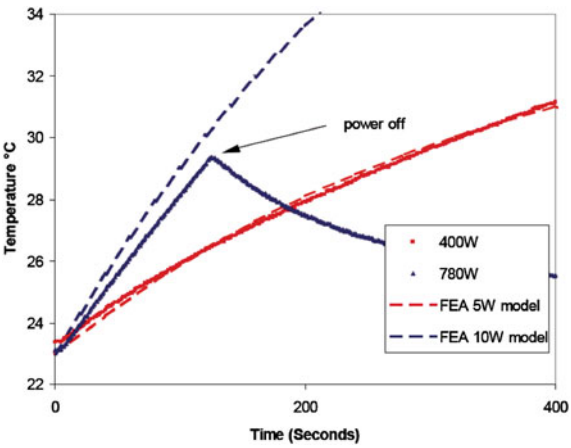

Fig. 24 Experimental maximum device temperature and modelled behaviour based on 5 and 10 W dissipated power

little difference between the two curves since the thermal behaviour is dominated by heat removal rather than heat generation. The form of the measured temperature rise in Fig. 25 is skewed towards the horn side, whereas the modelled temperature profile is roughly symmetric. These are transient curves, after 400 s operation.

Under steady state conditions the modelled temperature profile skews towards the end mass because of the reduced energy removal from this component, thus increasing the discrepancy between measured and modelled behaviour. It is clear that although the model may be used to predict approximate temperatures there are still discrepancies between modelled and measured behaviour. In order for the temperature profile to skew as seen experimentally, there must be less heat removal from the horn end. This could be because of inaccurate thermal properties for this material, or more likely due to thermal contact resistance between the ceramic and the horn. The initial FEA model has assumed that the six PZT pieces are one solid piece, and that there is perfect contact between the ceramic and the end mass, and the ceramic

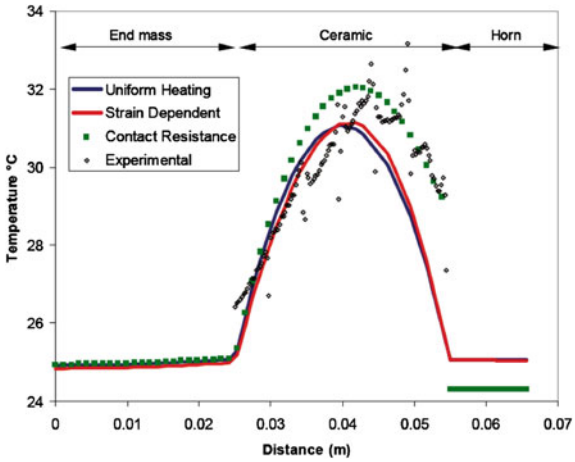

Fig. 25 Experimental temperature profile compared to FEA models based on dielectric heating, *blue line*, and strain heating model, *red line*, with added contact resistance, *green*

and the horn. If a thermal contact resistance element is placed between the ceramic and the horn, then a skew of the temperature profile similar to that seen experimentally is observed. The contact resistance is characterised by a thermal contact conductance (TCC) such that the heat flux per unit area across the contact is TCC multiplied by the temperature difference across the contact. A value of 250 W/m^2K for the thermal contact conductance gave the green trace in Fig. 25, where a value of 5000 W/m^2K is a 'perfect' contact. The model could be improved by adding the various extra interfaces, however it does mean that accurate values for these contact resistances would be needed.

Conclusion

A finite element model enables more complex geometries to be considered, and realistic results can be obtained. Using the heat generation values based on the dielectric heating model, obtained using input parameters of applied voltage, material permittivity and tan δ_e, gives acceptable results. The added complexity of space dependent heat generation does not give significantly different results, since unbalanced heat removal rather than heat generation dominates the behaviour in this system. For this particular transducer it appears that contact resistance at the component interfaces plays a significant part in controlling the temperature rise. Practically, the system cannot be run at high power levels without adequate convective cooling, however the temperature rise in the current configuration might be reduced by careful selection and manufacturing of the interfaces between the various components.

6 Concluding Comments

Failures due to thermal issues are common in high power piezoelectric devices. This chapter gives engineers an understanding of the problems, where they occur and how to avoid them. The work covers methods used to predict the temperature rise seen, based on simple analytical models and the use of Finite Element Models.

The case studies illustrate the use of these methods in examples that embody most of the conditions seen in real systems. The input data required in these simulations were measured using the methods describe in the chapter annexes.

Appendix A: Thermal Property Data of Piezoelectric Materials

In order to be able to make any predictions of how a piezoelectric device will perform in terms of self induced temperature rise, some knowledge of the thermal properties are needed, typically the thermal conductivity k, but also the thermal diffusivity α, and the specific heat capacity Cp. Data for these properties is scarce in the literature, with the most often quoted source coming from Berlincourt et al. [36], where a single value for thermal conductivity and specific heat capacity is given for all PZT materials with no information regarding the temperature dependence.

A.1 Specific Heat Capacity, C_p (J/kg K)

The specific heat capacity, C_p, is the amount of energy needed to raise the temperature of 1kg of the material by one degree. This can be used to determine the temperature rise of a volume of a material since the change in energy stored is proportional to the specific heat through the following equation;

$$\dot{E}_{st} = \frac{d}{dt}(\rho V C_p T) \tag{28}$$

where ρ and V are the density and volume of the material. If the internal power generation rate of the material is known, then the resultant temperature rise can be determined.

As discussed the most quoted value for the specific heat capacity of PZT is 420 J/kgK [36], but Table 2 gives a summary of other sources that give values for the room temperature value ranging from 350 to 491 J/kg K. Yarlagadda et al. [37] made a comprehensive set of measurements of heat capacity and thermal conductivity over the temperature range 20–300 K and show that the specific heat capacity varies greatly over this range, and is different for hard and soft materials. The soft material PZT-5H increases 15 fold over the temperature range, whilst the hard composition only increases by around 4 times. These values are not necessarily inconsistent with

Table 2 Specific Heat Capacity values for PZT type piezoelectric materials

Material	Temperature (K)	Specific heat capacity (J/kg K)	References
PZT 5H	22	23.3	[37]
PZT 5H	155	348	[37]
PZT 4S	22	42.6	[37]
PZT 4S	155	159	[37]
PZT(TRS-600)	Room	413*	[38]
PMN-PT-BT	Room	350	[30]
PZT	Room	420	[36]
Modified barium titanate	Room	500	[36]
PZT [MT-18]	Room	491	[22]
PZT	Room	350	[39]
PZT	Room	320**	[40]

*Value quoted as volume specific heat capacity, 3.26 × 106 J/m3 °C, using a density of 7900 kg/m^3 to convert to specific heat capacity

** Value quoted as volume specific heat capacity, 2.5 × 106 J/m^3 °C, using a density of 7900 kg/m^3 to convert to specific heat capacity

the room temperature values reported in the literature as some of the temperature dependence may be due to phase changes, indeed the authors attribute deviations at around 50–80 K to transition type behaviour.

The most common operating regime for piezoelectric actuators is from ambient temperature to around 300 °C and there is little published information on the change in specific heat over this temperature range. Measurements of the specific heat capacity of a soft and a hard PZT composition were made at NPL, from room temperature to 200 °C, using a Perkin Elmer DSC 7 Differential Scanning Calorimeter. The basis of DSC measurements is that a sample of known weight is placed in a holder, and the amount of energy provided by an electrical heater, which is required to increase the temperature of the sample per degree is measured. The test is carried out at a constant heating rate during which the heater power is adjusted continuously to compensate for heat absorbed or evolved by the sample, to keep the sample holder temperature identical to that of the reference holder. The energy input by the electrical heater is measured and this is proportional to the specific heat.

Measurements were repeated on two samples of each composition and the results are plotted in Fig. 26. The room temperature values are the order of 20 % lower than the most often quoted value, although they do increase by approximately 15 % over the measured temperature range. The soft material has a slightly higher specific heat capacity than the hard, but the difference is not much greater than the sample-to-sample variation.

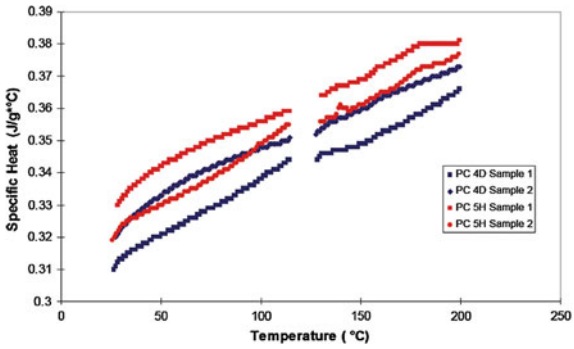

Fig. 26 Specific heat variation with temperature, for PZT 4D and PZT 5H

A.2 Thermal Conductivity, k (W/m K)

In order to determine the equilibrium state of a device, i.e. a steady state thermal solution, only the thermal conductivity of the material is required, which has units W/m K. Thermal conductivity is defined as the rate at which heat flows through a certain area of a body. The precise definition is given by Fourier's equation:

$$\frac{dq}{dt} = -kA\frac{dT}{dx} \tag{29}$$

where q is the heat energy flowing in the x direction through the area, A during time, t. dT/dx is the temperature gradient, and k is the thermal conductivity of the material.

Table 3 summarises the published values of thermal conductivity of PZT type piezoelectric materials, where values range from 0.8 to 2.3 W/m K. Again Yarlagadda et al. [37] have determined the thermal conductivity below 300 K and found that PZT-4S was almost twice as conductive as PZT-5H, and that there is a significant temperature dependence, however their room temperature thermal conductivity results fall well below the generally accepted value of between 1 and 2 W/mK. In general most thermal models assume the thermal conductivity is temperature independent, most probably because of a lack of published data on the temperature dependence.

A.2.1 Errors

As can be seen from Table 3, the published values of thermal conductivity varies by around 100 %, and the errors in the measured value will be reflected in the predicted thermal behaviour, depending on the exact details of the case. In general the errors in the thermal conductivity are propagated linearly to the results. For example, Sherrit et al. [24] predict an internal temperature rise of 36 °C in a 20 mm diameter, 2 mm thick disc, using a value of k = 1.25 W/m K, however this will be reduced to 23 °C when

Table 3 Thermal conductivity values for PZT type piezoelectric materials

Material	Temperature K	Thermal conductivity (W/mK)	References
PZT-4D	Room	1.8	[32]
PZT	Room	2.3*	[41]
PZT 5H	15	0.01	[37]
PZT 5H	300	0.14	[37]
PZT 4S	15	0.018	[37]
PZT 4S	300	0.34	[37]
PZT	Room	1.0–1.5	[25]
PMN-PT-BT	Room	3.59	[30]
PZT-4S	Room	2.1	[42]
PZT	Room	1.25	[36]
Modified Ba Titanate	Room	2.5	[36]
PZT[MT-18]	Room	1.5	[3]
PZT	Room	1.1	[39]
PZT	Room	0.8	[40]
PZT 4	Room	2.0	[43]
PMN-PT single crystal	20	0.2	[44]
PMN-PT single crystal	320	2.6	[44]

* published value 23, but presumed to be a typographical error

a value of $k = 2$ W/m K is used. This is evident from the first term in Eq. (15) where the temperature rise is proportional to the reciprocal of the thermal conductivity. In contrast, Hu [25] has shown that varying the thermal conductivity from 1 to 1.5 W/m K has little effect on the predicted temperature rise, and that power input was the dominant factor in modelling temperature rise in piezoelectric transformers.

A.3 Thermal Diffusivity, α (m^2/s)

Thermal diffusivity is the material property governing heat flow when the temperature is varying with time, and has the dimension length^2/time, with units of m^2/s. The thermal diffusivity can be determined experimentally, and it is related to the thermal conductivity k, through the following relationship

$$\alpha = \frac{k}{\rho \cdot C_p} \tag{30}$$

where ρ is the density and C_p is the specific heat capacity.

Using the published values for k, ρ and C_p the thermal diffusivity of PZT is around 5×10^{-7}m^2/s. Lang [45] has measured the thermal diffusivity of bulk piezoelectric materials using the Laser Intensity Modulation Method (LIMM), and obtained values close to this estimate, Table 4.

Table 4 Thermal diffusivity values for PZT type piezoelectric materials

Material	Temperature (K)	Thermal diffusivity (m^2/s)	References
PZT (Plessey RM200)	Room	4.59E-7	[45]
PSZT	Room	4.53E-7	[45]

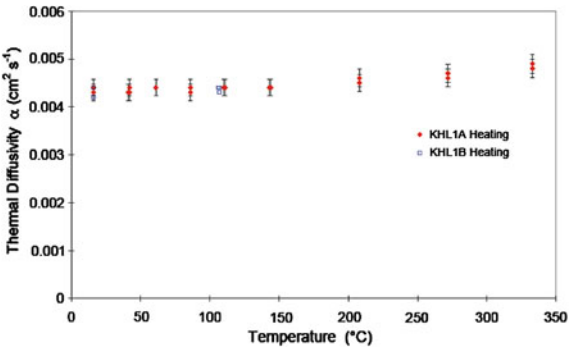

Fig. 27 Thermal diffusivity measurements of PZT-5H using laser flash

The thermal diffusivity of PZT was also measured at NPL, using a Netzsch Laser Flash 427. The measurement involves heating the front face of a disc-shaped sample of known dimensions, usually 12.5 mm diameter and 1.5–2.5 mm thickness using a high intensity Nd:YAG laser with a pulse width of between 0.2 and 1.2 ms. The temperature rise on the rear face is monitored using an InSb infrared detector. From the temperature rise with time, the thermal diffusivity can be calculated, applying appropriate corrections for radiation and the finite laser pulse length. Because of limited samples of the correct dimension only a soft PZT 5H composition was measured. The measured value for the thermal diffusivity of PZT-5H was around 4.5×10^{-7} m^2/s, with little measurable change over the range room temperature to 350 °C, this compares favourably with measured values reported in the literature, Fig. 27.

The thermal conductivity can also be derived from the measured thermal diffusivity and the measured values of specific heat capacity, and lie between 1.1 and 1.3 W/mK over the temperature range room temperature to 200 °C.

Acknowledgments This work was supported by the UK's National Measurement System programme—Measurement for Materials Processing and Performance, MPP. Thanks are also due to T Amato, (PURAC), F Rawson (FFR Ultrasonics Ltd.) and D Hazelwood (R&V Hazelwood Associates) for the loan of equipment, support and advice.

References

1. Berlincourt, D., Krueger H., Near C.: Technical publication TP-226 properties of Morgan Electro ceramic ceramics. Morgan Electro Ceramics, vol. 12. (2003)
2. Tokin, N.: Multileyer Piezoelectric Actuators. NEC/TOKIN vol. 07

3. Merker, U., Droste, E., Michaelis, A.: Thermal Runaway of Tantalum Capacitors, pp. 102–106. CARTS, Europe (2002)
4. Richard, C., Lee, H.S., Guyomar, D.: Thermo-mechanical stress effect on 1–3 piezocomposite power transducer performance. Ultrasonics **42**(1–9), 417–424 (2004)
5. Mitrovic, M., Carman, G., Straub, F.K.: Durability properties of piezoelectric stack actuators under combined electromechanical loading. Proc. SPIE **3992**, 217 (2000)
6. Takahashi, S., Sasaki Y., Hirose, S.: Driving electric field effects on piezoelectric transducers. Jpn. J. Appl. Phys. **36**(1), 3010–3015 (1997)
7. Technical Publication TP-221 Piezoelectric CeramicsVisit the Morgan Electro Ceramics. Web Site: www.morganelectroceramics.com. Power Capacities of Piezoelectric Ceramics in Sonar-type Acoustic Transducers. pp. 1–8, (1999)
8. Hu, J., Ho, S.-F., Ong, E.-L., Du, J.: An experimental investigation of the temperature field in small piezoelectric vibrators. Ultrasonics **41**(9), 731–735 (2004)
9. Uchino, K., Hirose, S.: Loss mechanisms in piezoelectrics: how to measure different losses separately. IEEE Trans. Ultrason. Ferroelectr. Freq. Control **48**(1), 307–321 (2001)
10. Richard, C., Goujon, L., Guyomar, D., Lee, H.S., Grange, G.: Selecting passive and active materials for 1.3 composite power transducers. Ultrasonics **40**(1), 895–901 (2002)
11. Lente, M., Eiras, J.: Interrelationship between self-heating and ferroelectric properties in PZT ceramics during polarization reorientation. J. Phys. Condens. Matter **12**, 5939 (2000)
12. Ronkanen, P., Kallio, P., Vilkko, M., Koivo, H.: Self heating of piezoelectric actuators: measurement and compensation. In: Proceedings of the 2004 International Symposium on Micro-Nanomechatronics and Human Science, 2004 and the Fourth Symposium Micro-Nanomechatronics for Information-Based Society, 2004, pp. 313–318 (2004)
13. Mignogna, R.B., Green, R.E., Duke, J.C., Henneke, E.G., Reifsnider, K.L.: Thermographic investigation of high-power ultrasonic heating in materials. Ultrasonics **19**(4), 159–163 (1981)
14. Incropera, F.P., DeWitt, D.P.: Fundamentals of Heat and Mass Transfer. Wiley, New York (1996)
15. Tashiro, S., Ikehiro, M., Igarashi, H.: Influence of temperature rise and vibration level on electromechanical properties of high-power piezoelectric ceramics. Jpn. J. Appl. Phys. **36**(1), 3004–3009 (1997)
16. Jordan, T., Qunaies, Z.: Piezoelectric ceramics characterization. Technical Report 2001–28 (2001)
17. Jordan, T.: Langley Research Center, U. S. N. A. Administration, and Space. Electrical properties and power consideration of a piezoelectric actuator (2000)
18. Zhang, Q.M., Wang, H., Zhao, J.: Effect of driving field and temperature on the response behaviour of ferroelectric actuator and sensor materials. J. Intell. Mater. Syst. Struct. **6**, 84–93 (1995)
19. Hooker, M., Langley Research Center: Properties of PZT-based piezoelectric ceramics between -150 and 250C. Technical Report (1998)
20. Gdula, R.A.: High field losses of adulterated lead zirconateG titanate piezoelectric ceramics. J. Am. Ceram. Soc. **51**(12), 683–687 (1968)
21. Berlincourt, D.A.: Clevite: Power Limitations of piezoelectric ceramics in radiating transducers (Technical paper TP-225). Piezoelectric Division/Clevite Corp. (1962)
22. Ando, E., Kagawa, Y.: Finite-element simulation of transient heat response in ultrasonic transducers. IEEE Trans. Ultrason. Ferroelectr. Freq. Control **39**(3), 432–440 (1992)
23. Lu, X., Hanagud, S.V.: Extended irreversible thermodynamics modeling for self-heating and dissipation in piezoelectric ceramics. IEEE Trans. Ultrason. Ferroelectr. Freq. Control **51**(12), 1582–1592 (2004)
24. Sherrit, S., Bao, X., Sigel, D.A., Gradziel, M.J., Askins, S.A., Dolgin, B.P., Bar-Cohen, Y.: Characterization of transducers and resonators under high drive levels. Ultrasonics Symposium, 2001 IEEE, vol. 2, pp. 1097–1100 (2001)
25. Hu, J.: Analyses of the temperature field in a bar-shaped piezoelectric transformer operating in longitudinal vibration mode. IEEE Trans. Ultrason. Ferroelectr. Freq. Control **50**(6), 594–600 (2003)

26. Kanayama, K.: Thermal analysis of a piezoelectric transformer. Ultrasonics Symposium, 1998, Proceedings., 1998 IEEE, vol. 1. pp. 901–904 (1998)
27. Piezoelectric properties of ceramic materials and components: Part 3: Methods of measurement: High power. BS En 50234–3 (2002)
28. Carslaw, H.S., Jaeger, J.C.: Conduction of Heat in Solids, Ser. Oxford science publications, Clarendon Press, New York (1959)
29. Stulen, F., Senapati, N., Gould, R.: Temperature distribution in an ultrasonic power transducer. Ultrason. Int. **83**, 301–306 (1983)
30. Shankar, N., Hom, C.: An acoustic/thermal model for self-heating in PMN sonar projectors. J. Acoust. Soc. Am. **108**, 2151 (2000)
31. Robinson, H.: Large signal dielectric losses in electrostrictive materials. Proc. SPIE **3992**, 91 (2000)
32. Abboud, N., Mould, J., Wojcik, G., Vaughan, D., Powell, D., Murray, V. MacLean, C.: Thermal generation, diffusion and dissipation in 1–3 piezocomposite sonar transducers: finite element analysis and experimental measurements. Ultrasonics Symposium, 1997. Proceedings., 1997 IEEE, vol. 2. pp. 895–900 (1997)
33. Zheng, J., Takahashi, S., Yoshikawa, S., Uchino, K., Vries, J.d.: Heat generation in multilayer piezoelectric actuators. J. Am. Ceram. Soc. **79**(12), 3193–3198 (1996)
34. Yao, K., Uchino, K., Xu, Y., Dong, S., Lim, L.C.: Compact piezoelectric stacked actuators for high power applications. IEEE Trans. Ultrason. Ferroelectr. Freq. Control **47**(4), 819–825 (2000)
35. Pritchard, J., Ramesh, R., Bowen, C.R.: Time-temperature profiles of multi-layer actuators. Sens. Actuat. A: Phys. **115**(1), 140–145 (2004)
36. Mason, W.P., Thurston, R.N.: Physical Acoustics: Principles and Methods, ser. Physical Acoustics. Academic Press, New York (1976)
37. Yarlagadda, S.: Low temperature thermal conductivity, heat capacity and heat generation of PZT. J. Intell. Mater. Syst. Struct. **6**, 757 (1995)
38. Weiland, L.M., Lynch, C.S.: Thermo-electro-mechanical behavior of ferroelectric materials part II: Introduction of rate and self-heating effects. J. Intell. Mater. Syst. Struct. **14**(10), 605–621 (2003)
39. P. I. Ceramic. Piezoelectric Ceramics Products, PI Ceramic GmbH. http://www.piceramic.com
40. Bauer, S., Ploss, B.: A method for the measurement of the thermal, dielectric, and pyroelectric properties of thin pyroelectric films and their applications for integrated heat sensors. J. Appl. Phys. **68**(12), 6361 (1990)
41. Zhou, S.W., Rogers, C.A.: Heat generation, temperature, and thermal stress of structurally integrated piezo-actuators. J. Intell. Mater. Syst. Struct. **6**(3), 372–379 (1995)
42. Lesieutre, G.A., Fang, L., Koopmann, G.H., Pai, S.P., Yoshikawa, S.: Heat generation of a piezoceramic induced-strain actuator embedded in a glass/epoxy composite panel. 1996 Symposium on Smart, Structures and Materials, pp. 267–275 (1996)
43. Dubus, B., Boucher, D.: An analytical evaluation of the heating of lowGfrequency sonar projectors. J. Acoust. Soc. Am. **95**, 1983 (1994)
44. Zhu, D., Han, P.: Thermal conductivity and electromechanical property of single-crystal lead magnesium niobate titanate. Appl. Phys. Lett. **75**, 3868 (1999)
45. Lang, S.: Technique for the measurement of thermal diffusivity based on the laser intensity modulation method (LIMM). Ferroelectrics **93**(1), 87–93 (1989)